Asociación Argentina
de Mecánica Computacional

Mecánica Computacional Vol XXXIII, págs. 691-703 (artículo completo)
Graciela Bertolino, Mariano Cantero, Mario Storti y Federico Teruel (Eds.)
San Carlos de Bariloche, 23-26 Setiembre 2014

DYNAMICS OF MAGNETIC RELAXATION INSIDE A CYLINDRICAL FLUX CONSERVER

Pablo L. García-Martínez[a,b], Leandro G. Lampugnani[a] and Ricardo Farengo[c]

[a]*CONICET, Gerencia de Física - Centro Atómico Bariloche, Av. Bustillo 9500 (8400) S.C. de Bariloche - Río Negro, Argentina, http://www.comahue-conicet.gob.ar/*

[b]*Universidad Nacional de Río Negro - Sede Andina, Mitre 630 (8400) S.C. de Bariloche - Río Negro, Argentina, http://sedeandina.unrn.edu.ar/*

[c]*CNEA - Instituto Balseiro, Gerencia de Física - Centro Atómico Bariloche, Av. Bustillo 9500 (8400) S.C. de Bariloche - Río Negro, Argentina, http://fisica.cab.cnea.gov.ar/*

Keywords: Magnetohydrodynamics, Plasma Relaxation, Magnetic Reconnection, Self-Organization, Finite-Volume Method.

Abstract. Rapid localized magnetic reconnection events within a magnetohydrodynamic (MHD) unstable plasma produce rapid dissipation of magnetic energy while leaving system's global magnetic helicity almost unaffected. This is the basis of a robust principle called magnetic relaxation. When the plasma is bounded by flux conserving walls, magnetic relaxation induces the spontaneous formation of large scale coherent magnetic structures (plasma self-organization). In this work, the dynamics of magnetic relaxation inside a simply connected volume (a cylinder) is studied by solving the visco-resistive MHD system of equations in three spatial dimensions. The discretization of the governing equations is performed with the finite-volume method and a high resolution total-variation-diminishing (TVD) solver is employed to treat non linearities. The formation and sustainment of a toroidal configuration, known as spheromak, inside the simply connected domain is demonstrated. A set of boundary conditions that correctly models the injection of magnetic energy and helicity, required to balance resistive dissipation, is described. Different initial conditions are tested and their impact on the final quasi-steady state is discussed. In particular, we show that it is possible to sustain the so called "flipped" spheromak. The MHD activity in both cases (normal and flipped) is studied.

1 INTRODUCTION

The macroscopic dynamics of high temperature plasmas occurring in space or at the laboratory is well described by the magnetohydrodynamics (MHD) model. In this framework, the plasma is regarded as a conducting fluid having electrical resistivity and viscosity. Since these dissipative effects are typically small (i.e. large Reynolds and magnetic Reynolds numbers), it is common to find extremely complex behavior (e.g. turbulence), due to the non-linear dynamics of the fluid which is strongly coupled with that of the magnetic field. It is therefore remarkable that one can make quantitative predictions about the plasma configuration resulting from such complex behavior. This is possible because localized MHD fluctuations allow the plasma to rapidly access to a particular minimum-energy state. This process, known as plasma relaxation, involves the reconnection of magnetic field lines and is an important example of the self-organization of a complex system (Hasegawa, 1985).

An important concept in the theory of plasma relaxation is that of global magnetic helicity, $H = \int_V \mathbf{A} \cdot \mathbf{B}\, d^3r$ (where $\mathbf{A}$ is the vector potential of the magnetic field $\mathbf{B}$), which is, like magnetic energy $W = \frac{1}{2}\int_V B^2\, d^3r$, an ideal invariant of motion. The relaxation theory is built on the following ansatz introduced by Taylor (1974): in a turbulent plasma with a small amount of dissipation, these two invariants decay at very different rates because localized magnetic reconnection events are able to rapidly dissipate magnetic energy while leaving global magnetic helicity almost unaffected. Thus, the plasma is expected to evolve towards a state of minimum magnetic energy under the constraint of magnetic helicity conservation. This can be formulated as variational problem whose solution is a linear force-free field that was already found by Woltjer (1958) in a different (astrophysical) context.

While this theory describes quite well the final state of low-β plasmas (β measures the ratio of pressure forces to magnetic forces) such as the reversed field pinch (RFP), the spheromak and other laboratory configurations (Taylor, 1986) as well as magnetic structures in the solar corona (Heyvaerts and Priest, 1984), it does not provide any information on how these configurations are formed. Furthermore, once formed these configurations need to be sustained against resistive dissipation. The dynamics of magnetic relaxation during sustainment is highly relevant to several confinement experiments involving fusion plasmas and is out of the scope of the relaxation theory.

In this paper we present a numerical study of the dynamics of magnetic relaxation inside a cylindrical flux conserver while magnetic helicity is being injected by tangential boundary flows at the magnetic flux inlet. The feasibility of forming and sustaining a spheromak configuration with this helicity injection mechanism has already been shown (García Martínez and Farengo, 2010). In this work we focus on the dynamics of the saturated states obtained from different initial conditions, for the same set of boundary conditions. In particular, we show that it is possible to sustain the so called "flipped" spheromak. In Sec. 2 the theory of relaxation in driven configurations is briefly introduced and the motivation of this work is explained. The system of equations that model the dynamics as well as the numerical approach are presented in Sec. 3. The results are discussed in Sec. 4. Finally, the conclusions are summarized in Sec. 5.

2 RELAXATION IN DRIVEN CONFIGURATIONS

The minimum energy-state for a given amount of magnetic helicity, i.e. the relaxed state, is the magnetic configuration that satisfies

$$\nabla \times \mathbf{B} = \lambda \mathbf{B} \tag{1}$$

with constant λ. Rosenbluth and Bussac (1979) showed that the relaxed state inside a spherical flux conserver is an axisymmetric system of nested toroidal magnetic surfaces, that they called "spheromak".

We want to study relaxation inside a cylindrical flux conserver where the relaxed state is also axisymmetric. In such case it is convenient to rewrite Eq. (1) in terms of the poloidal flux function defined as

$$\psi(r,z) = \int_{S(r,z)} \mathbf{B} \cdot d\mathbf{s} \tag{2}$$

were $S(r,z)$ is the circle of radius r centered at the position z of the vertical axis (see Fig. 1). In this geometry the poloidal plane is the r-z plane and the toroidal direction is that of the azimuthal angle ϕ. Note that surfaces of constant ψ are magnetic flux surfaces and that ψ acts as a stream function for the poloidal magnetic field. In terms of the poloidal flux, the force-free equilibrium Eq. (1) becomes

$$-\Delta^* \psi = \lambda^2 \psi \tag{3}$$

where $\Delta^* = \partial^2/\partial r^2 - (1/r)\partial/\partial r + \partial^2/\partial z^2$ is the Grad-Shafranov operator (see García Martínez (2012) for further details). This equation may describe two different problems depending on the imposed boundary conditions: isolated configurations for homogeneous boundary conditions and driven configurations for non-vanishing ψ at the flux conserver's walls.

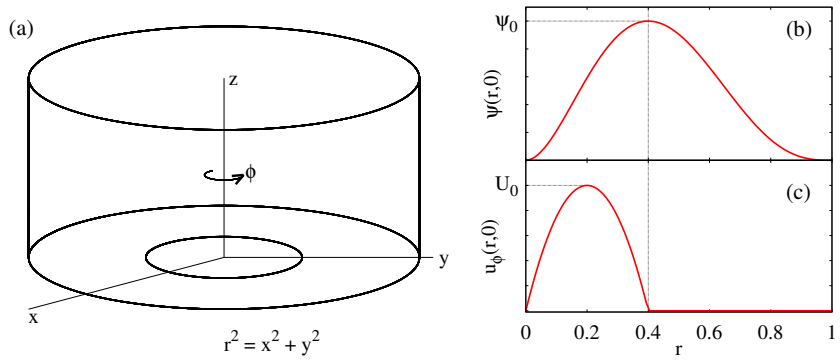

Figure 1: Geometry of the domain and boundary conditions.

When isolated configurations are considered, ψ vanishes at the boundary and Eq. (3) represents an eigenvalue problem that only has solution for discrete λ_n eigenvalues. Note that the eigenvalues are fully determined by the geometry of the domain. For example, in the case of a cylinder the lowest eigenvalue turns out to be

$$\lambda_1 = \sqrt{\frac{x_{11}^2}{a^2} + \frac{\pi^2}{h^2}}. \tag{4}$$

where x_{11} is the first zero of the Bessel function J_1 and a and h are the cylinder radius and height respectively. The relaxed state regarded as the lowest eigenstate of the plasma in an isolated flux conserver was the original framework of relaxation theory (Taylor, 1974; Rosenbluth and Bussac, 1979).

In later works, the scope of relaxation theory was extended to include driven configurations (Jensen and Chu, 1984). In order to inject magnetic energy and helicity to the system, magnetic field lines intercepting the boundary must exist. Thus, some magnetic flux has to cross the

boundary and $\psi \neq 0$ there. The regions of the boundary in which $\psi \neq 0$ are called electrodes. With non-homogeneous boundary conditions, Eq. (3) has a solution for each λ value, excepting at the eigenvalues λ_n, where the solution diverges. In this case, the continuous λ value is set by the external source as explained below.

Let's consider the particular case of a cylindrical flux conserver with $a = h = 1$ and concentric electrodes at its base, as shown in Fig.1 (a). Due to axisymmetry, the problem reduces to solve Eq. (3) in the rectangle $[0, 1] \times [0, 1]$ of the r-z plane. The boundary condition is $\psi = 0$ everywhere, excepting at $z = 0$, where we impose

$$\psi(r, 0) = C\psi_0(r)^2(1 - r)^3, \tag{5}$$

with $C = 28.935$, as shown in Fig. 1 (b). This profile models an external solenoid that injects a magnetic flux of strength ψ_0 across the circle $r < 0.4$. This flux leaves the chamber through the annular region $0.4 < r < 1$ (Brennan et al., 2002). When the external source is such a solenoid and no current is driven along the magnetic field lines, the externally imposed λ is equal to zero. This corresponds to the vacuum magnetic field shown in Fig. 2 (a). Note that all the magnetic field lines are "open", i.e. they close outside the domain.

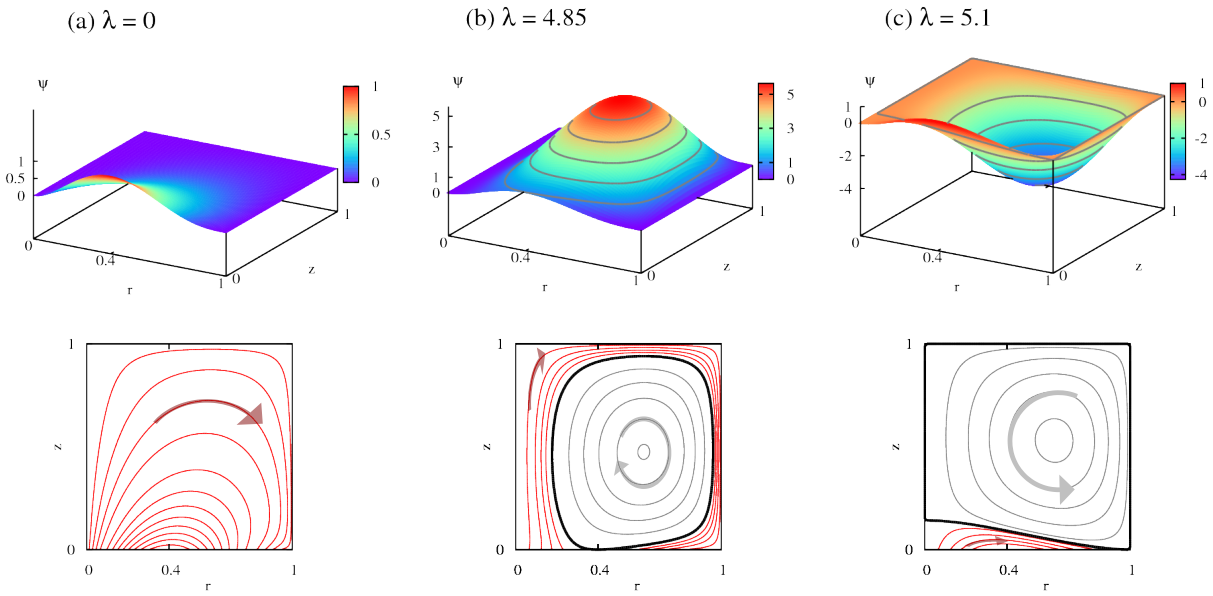

Figure 2: Force-free equilibria with external driving for different values of λ: (a) $\lambda = 0$ current-free vacuum solution, (b) $\lambda = 4.85$ regular spheromak and (c) $\lambda = 5.1$ flipped spheromak (post-resonance). These solutions were used as initial conditions for the MHD simulations.

In order to inject magnetic helicity, electric current must be driven along the magnetic field. In the present description of the problem, this is done by increasing the λ value. When $\lambda > 4$ the first closed magnetic surfaces appear. For $\lambda = 4.85$ we obtain the solution shown in Fig. 2 (b), which is representative of typical coaxial-helicity-injected (CHI) spheromaks. The open field lines are shown in red and the closed field lines are shown in gray. The outermost closed surface, called separatrix, is shown in black. The o-point where ψ achieves its maximum, ψ_a, is the magnetic axis of the configuration. The ratio ψ_a/ψ_0 is the flux amplification factor and is an important figure of merit of the configuration. The typical experimental values of ψ_a/ψ_0 lie between 4 and 5 (Jarboe, 2005).

As λ approaches the eigenvalue $\lambda_1 = 4.955$, computed from Eq. (4), the solution, as well as the flux amplification factor, diverges. For values above λ_1, ψ_a reverts its sign and a different configuration is obtained: the "flipped" spheromak. This is shown in Fig. 2 (c). In this case, the open flux does not wrap around the closed flux surfaces which seem to be detached from the source.

2.1 Limitations of the theory and motivation of this work

Despite its simplicity, the axisymmetric model just described provides a good description of the configurations obtained in experiments with coaxial plasma guns and other devices that are able to inject magnetic helicity in a simply connected flux conserver (Jarboe, 2005). In particular, it was found that some discharges in experiments designed to form and sustain regular spheromaks, ended up in flipped spheromak configurations that could also be sustained (Barnes et al., 1986). This is considered as further evidence of the robustness of the theory.

The formation of any of these configurations involves instabilities and strong MHD activity which induce the localized reconnection events required for plasma relaxation. Once the large scale axisymmetric configuration is formed, it can be further sustained by the continual support of magnetic helicity and energy to balance ohmic dissipation. However, this sustainment phase involves the conversion of the externally supplied poloidal current (along the open magnetic field lines) into the toroidal current flowing along the closed magnetic lines. Equivalently, this process is often regarded as a flux conversion mechanism, from toroidal to poloidal. Any such sustainment mechanism is called a dynamo. In the context of the study of the Earth's magnetic field generation, Cowling (1934) showed that it is impossible to have a steady-state axisymmetric MHD dynamo.

Spheromaks involve sustained axisymmetric equilibria having internal toroidal currents, a process that, as explained above, can not be axisymmetric. As will be shown in Section 4, the time-average of recurring non-axisymmetric instabilities provide the required dynamo action. The good confinement properties of an axisymmetric system will necessarily be diminished when the dynamo fields are non-axisymmetric. The essential question is to what extent this necessary but undesirable departure from axisymmetry can be tolerated (Bellan, 2000). The present work is a contribution to the basic understanding required to answer this question.

3 EQUATIONS AND NUMERICAL APPROACH

The plasma dynamics is modeled with the visco-resistive MHD equations in the zero-β limit (i.e. pressure forces are neglected). In non-dimensional form these equations are

$$\begin{aligned} \frac{\partial \mathbf{u}}{\partial t} + \mathbf{u}\cdot\nabla\mathbf{u} &= \frac{1}{\rho_0}\big(\mathbf{J}\times\mathbf{B}\big) + \frac{1}{Re}\nabla\cdot\Pi, \\ \frac{\partial \mathbf{B}}{\partial t} &= -\nabla\times\mathbf{E}, \\ \mathbf{E} &= -\mathbf{u}\times\mathbf{B} + \frac{1}{Re_m}\mathbf{J}, \\ \mathbf{J} &= \nabla\times\mathbf{B}, \\ \nabla\cdot\mathbf{B} &= 0 \end{aligned} \tag{6}$$

where $\Pi = (\nabla\mathbf{u} + \nabla\mathbf{u}^{\mathrm{T}}) - 2/3(\nabla\cdot\mathbf{u})$. The scales chosen are the flux conserver radius a, the external magnetic flux ψ_0 and the Alfvén velocity c_A. The current density is further rescaled to absorb the μ_0 factor (vacuum permeability) of the Ampère's law. With these scales the Reynolds

and magnetic Reynolds numbers are $Re = ac_A/\nu$ and $Re_m = ac_A/\eta$, respectively, where ν is the kinematic viscosity and η the electrical resistivity. For the computations presented in this work we took $Re = Re_m = 2 \times 10^4$.

The system (6) is solved employing a finite volume method with a total variation diminishing (TVD) approximate Riemann solver (Roe, 1981; Powell et al., 1999). The $\nabla \cdot \mathbf{B} = 0$ constraint is maintained using the projection method Toth (2000). A uniform Cartesian grid ($N_x \times N_y \times N_z = 100 \times 100 \times 50$) is used to advance the equations in time and a poloidal grid ($N_r \times N_z = 50 \times 50$) containing the Fourier coefficients of the toroidal decomposition is employed to analyze the results. Each toroidal mode is labeled with its wave-number n. This resolution ensures that numerical dissipation introduced by the TVD scheme remains small compared to physical dissipation associated to viscosity and resistivity (García Martínez and Farengo, 2009a,b).

The boundary conditions at the cylindrical flux conserver (see Fig. 1) are imposed using a high-order boundary treatment for Cartesian grid schemes (Forrer and Jeltsch, 1998; García Martínez and Farengo, 2009a). Perfectly conducting wall conditions $\mathbf{B} \cdot \mathbf{n} = 0$, $\mathbf{J} \times \mathbf{n} = 0$ and $\mathbf{u} = 0$ are imposed at the top ($z = 1$) and lateral wall ($r = 1$). At the electrode end ($z = 0$) the poloidal flux (constant during all the simulation time) is prescribed by Eq. (5) (the normal component of the magnetic field is easily computed from ψ). With these boundary conditions there is neither energy nor helicity flux across the boundary of the domain.

Imposing tangential flows at a boundary intercepted by magnetic flux may result in the injection of helicity as can be inferred from the balance of global magnetic helicity

$$\frac{dH}{dt} = -2 \int_V \eta \mathbf{J} \cdot \mathbf{B} dV - 2 \oint_{\partial V} [(\mathbf{A} \cdot \mathbf{B})(\mathbf{u} \cdot \mathbf{n}) - (\mathbf{A} \cdot \mathbf{u})(\mathbf{B} \cdot \mathbf{n})] dS. \tag{7}$$

Here, H is actually the relative magnetic helicity computed using a gauge invariant definition (Jensen and Chu, 1984; Finn and Antonsen, 1985). The last term on the right gives the helicity injection produced by motions of the foot-points of the open magnetic field. This process has been proposed as the dominant helicity transfer mechanism in the solar corona (Heyvaerts and Priest, 1984).

It is easy to show that, in our configuration, a rigid rotation at the bottom end of the cylinder does not inject helicity. To inject helicity, a differential rotation in the foot-points of the open field lines has to be imposed. In order to produce a net helicity transfer across the boundary, we impose a tangential boundary flow only in the zone where there is magnetic flux entering into the domain ($r < 0.4, z = 0$). The computations presented in this work have $u_r = u_z = 0$ and $u_\phi = U_0 \max[0, 25(0.4 - r)r]$, at $z = 0$ (see Fig. 1 (c)). This is the simplest profile that gives $u_\phi = 0$ at $r = 0$ and at $r = 0.4$, which is the point at which B_z changes its sign. This flow injects helicity because $A_\phi = \psi(r, 0)/(2\pi r)$ there.

4 RESULTS AND DISCUSSION

In this Section we present the results of three simulations. The mathematical model, numerical approach and boundary conditions were described in Sec. 3 and are common to the three cases studied. These simulations only differ in the initial condition, which is computed by solving Eq. (3) with the prescribed boundary condition for ψ at the electrodes and three different values of λ, as indicated in Table 1. The magnetic configurations shown in Fig. 2 are very similar to the three different initial conditions (there is a small deviation in λ, but they are qualitatively the same).

Since the magnetic flux is normalized with ψ_0, ψ_a gives directly the flux amplification factor. The evolution of the absolute value of ψ_a is shown in Fig. 3 for the three runs. In the three cases

	Vacuum	Regular	Flipped
λ	0	4.855	5.035
ψ_a	1	5.9	-7.5

Table 1: Parameters for initial conditions.

the system reaches a quasi-steady state after a transient phase. The vacuum solution begins with $\psi_a = 1$ which means that no closed magnetic surfaces exist. At $t \approx 50$, non-axisymmetric activity appears causing a strong poloidal flux amplification event. Since the imposed boundary conditions only inject toroidal magnetic flux, this event is a clear signature of the flux conversion mechanism.

This can also be observed in the evolution of ψ_a for the initially regular case (green line). When the non-axisymmetric activity is absent, the initial ψ_a decays due to resistivity. The combined action of the external driving of the tangential boundary flows and resistive dissipation destabilize the system. At $t \approx 80$ the dominant toroidal modes appear and a flux amplification events is produced. After that, the final steady-state is reached. Note that the vacuum and regular cases evolve toward the same quasi-steady state.

The initially flipped configuration has $\psi_a < 0$. Its sign is preserved during the whole simulation (Fig. 3, blue line) which means that the final configuration in the quasi-steady state is still a flipped spheromak. This can also deduced from Fig. 4. For an isolated relaxed state, it turns out that the eigenvalue λ_1 is equal to twice the ratio of magnetic energy to helicity. In Fig. 4 we plot $\langle\lambda\rangle \equiv 2W_{n=0}/H_{n=0}$, compared to the eigenvalue λ_1 of the cylinder. As expected from the theory of relaxation in driven configurations, the system does not cross the resonance, i.e. those cases with initial $\lambda < \lambda_1$ remain with $\langle\lambda\rangle < \lambda_1$ in the sustainment phase, and viceversa. Since the steady state reached by the initially vacuum and regular cases are almost the same, in what follows we only consider the sustainment phase of the regular and flipped configurations.

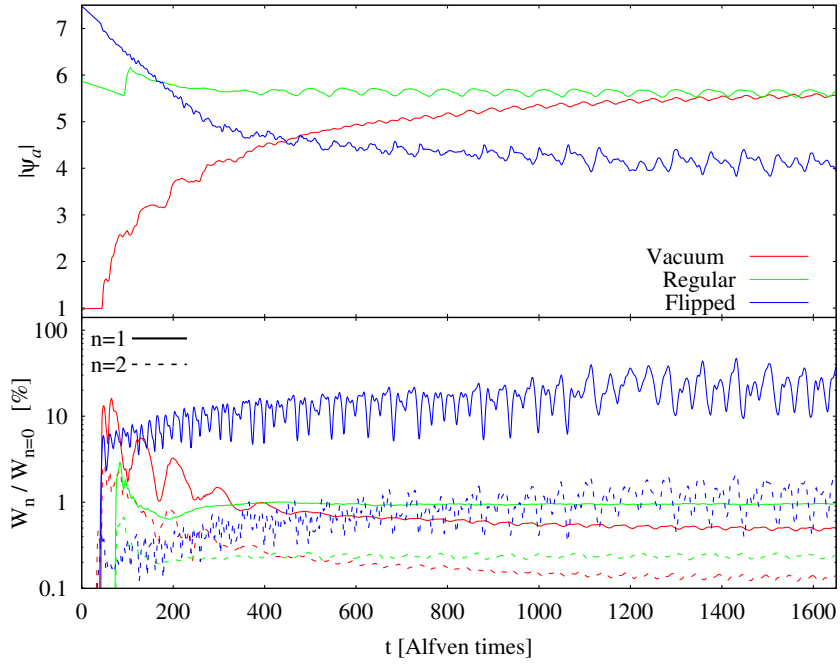

Figure 3: Evolution of $|\psi_a|$ and the magnetic energy content of the $n = 1$ and $n = 2$ toroidal modes (W_n), relative to the magnetic energy of the axisymmetric mode ($W_{n=0}$).

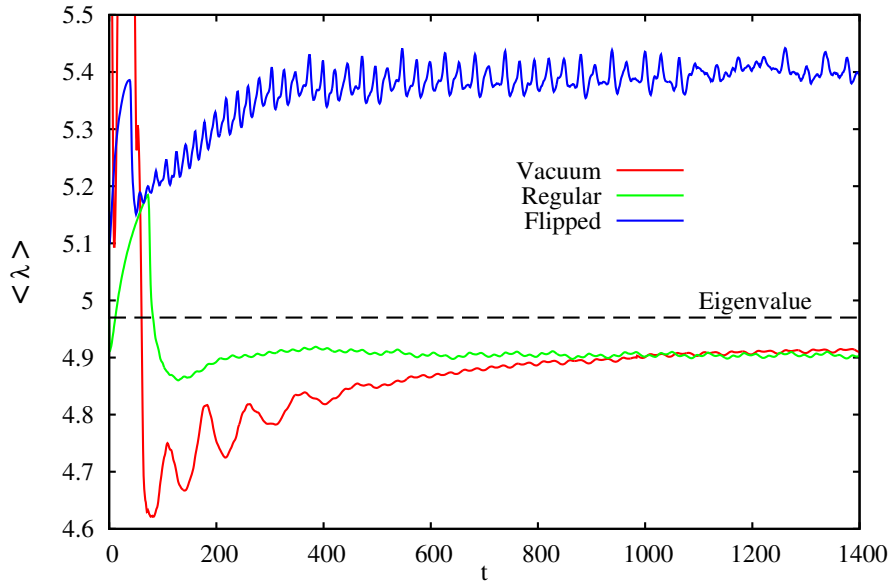

Figure 4: Evolution of $\langle\lambda\rangle = 2W_{n=0}/H_{n=0}$ for the three cases.

As explained in Sec. 2.1, the sustainment phase requires non-axisymmetric activity. The evolution of the relative amplitude (in magnetic energy) of the first two toroidal modes is shown in Fig. 3. In the regular case (as well as in the vacuum case) the fluctuations remain below 1% during sustainment. In contrast, sustainment of the post-resonance flipped configuration involves a higher level of fluctuations, in the order of 20%.

The spatial localization of the toroidal magnetic fluctuations, averaged during the sustainment phase, is shown in Fig. 5 for the regular and flipped cases. The mean magnetic configuration is shown by the contours of ψ, averaged during the sustainment phase ($1600 < t < 2000$). In the regular case, the fluctuations are highly localized in the open flux region (central flux column) while the flipped case shows a much larger region of closed surfaces that is affected by fluctuations. It is important to keep in mind that the contours of ψ do not coincide with

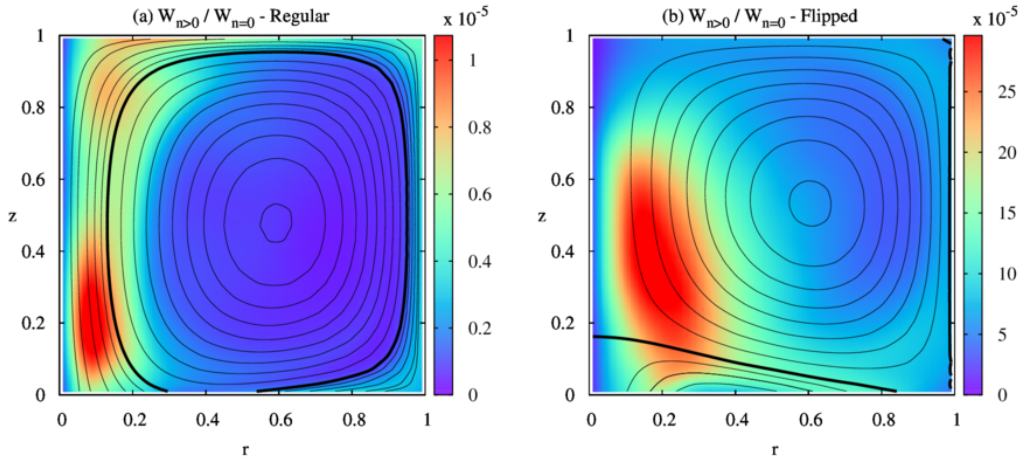

Figure 5: Average magnetic configuration (ψ contours) and spatial localization of the average fluctuations. Average is performed in the interval $1600 < t < 2000$.

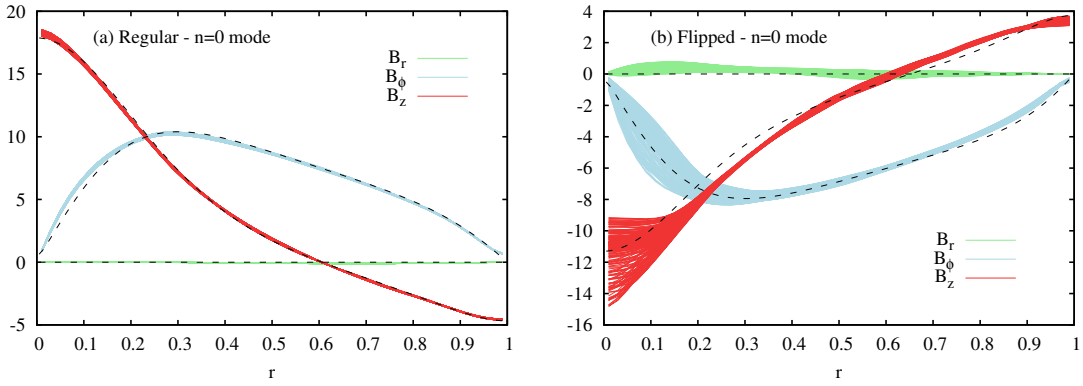

Figure 6: Fifty instantaneous radial profiles of the $n = 0$ magnetic field at the height of the mean magnetic axis, during sustainment.

magnetic flux surfaces when toroidal modes are present.

The mean magnetic configuration and its dispersion is shown in Fig. 6. The radial profiles of the three components of the magnetic field vector are plotted for fifty times during the sustainment phase. Only the axisymmetric $n = 0$ mode at the height of the magnetic axis, is used. The point at which B_z reverts its sign is the magnetic axis. The expected difference in the sign of the poloidal and toroidal components is observed. Also note that the absolute value of the magnetic field is smaller in the flipped case. A large dispersion of the $n = 0$ mode (over time) is observed for the flipped configuration, in agreement with the larger level of toroidal fluctuations.

From the discussion in Sec. 2 it is clear that the parameter λ plays a fundamental role in relaxation theory. Since the lowest energy state has uniform λ, it is expected that the system evolves towards that state. However, there is an inevitable deviation during sustain met and λ is not actually uniform in space. When that is the case, λ may be reinterpreted locally as the amount of current density parallel to $\mathbf{B}$ per unit of $\mathbf{B}$, i.e. $\lambda = \mathbf{J} \cdot \mathbf{B}/B^2$ (which may be readily

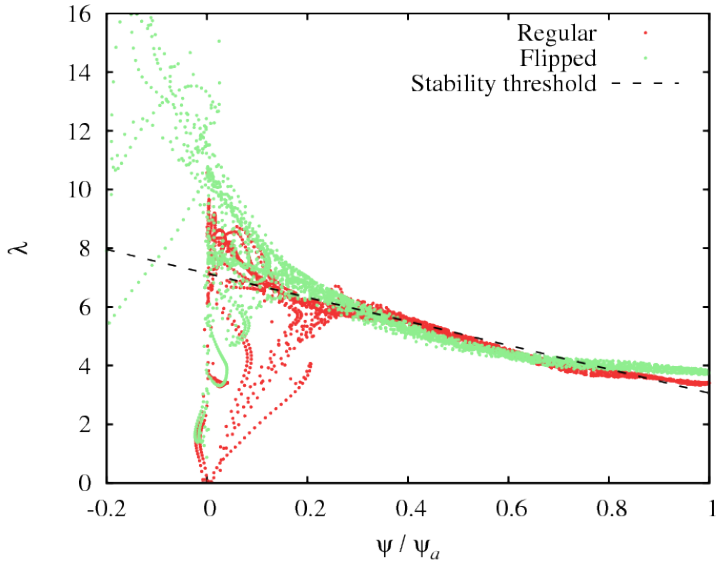

Figure 7: Local λ value at each poloidal position versus the poloidal flux, normalized with ψ_a. Averaged values during sustainment are used. Note that λ is approximately a function of ψ/ψ_a, for $\psi/\psi_a > 0.3$ and $\psi/\psi_a > 0.2$ for the regular and flipped cases respectively.

obtained from Eq. (1)).

In Fig. 7 the local λ at each poloidal position is plotted against the poloidal flux, normalized with ψ_a. Averaged values during sustainment are used. A clear deviation from the uniform λ relaxed state is observed. Furthermore, in the open flux region and near the separatrix ($\psi/\psi_a < 0.3$ for the regular case and $\psi/\psi_a < 0.2$ for the flipped case) a large dispersion of the λ values at each flux surface (i.e. at each ψ value) is observed. However, in the closed flux region, λ behaves as a function of ψ, in both cases. This means that, in average, the local value of λ is constant at each magnetic flux surface.

Experimental measurements have already shown that the sustained spheromak configuration is better approximated by a linear $\lambda(\psi)$ profile, than by the uniform λ fully relaxed state (Knox et al., 1986). Moreover, the stability analysis of the configuration shows a kink instability when the normalized slope of the $\lambda(\psi)$ profile is higher than -0.4 (Knox et al., 1986; García Martínez, 2012). This stability threshold is plotted in Fig. 7 (dashed line). It is interesting to note that both the regular and flipped configuration respect the same stability threshold. This λ gradient can not be predicted from relaxation theory.

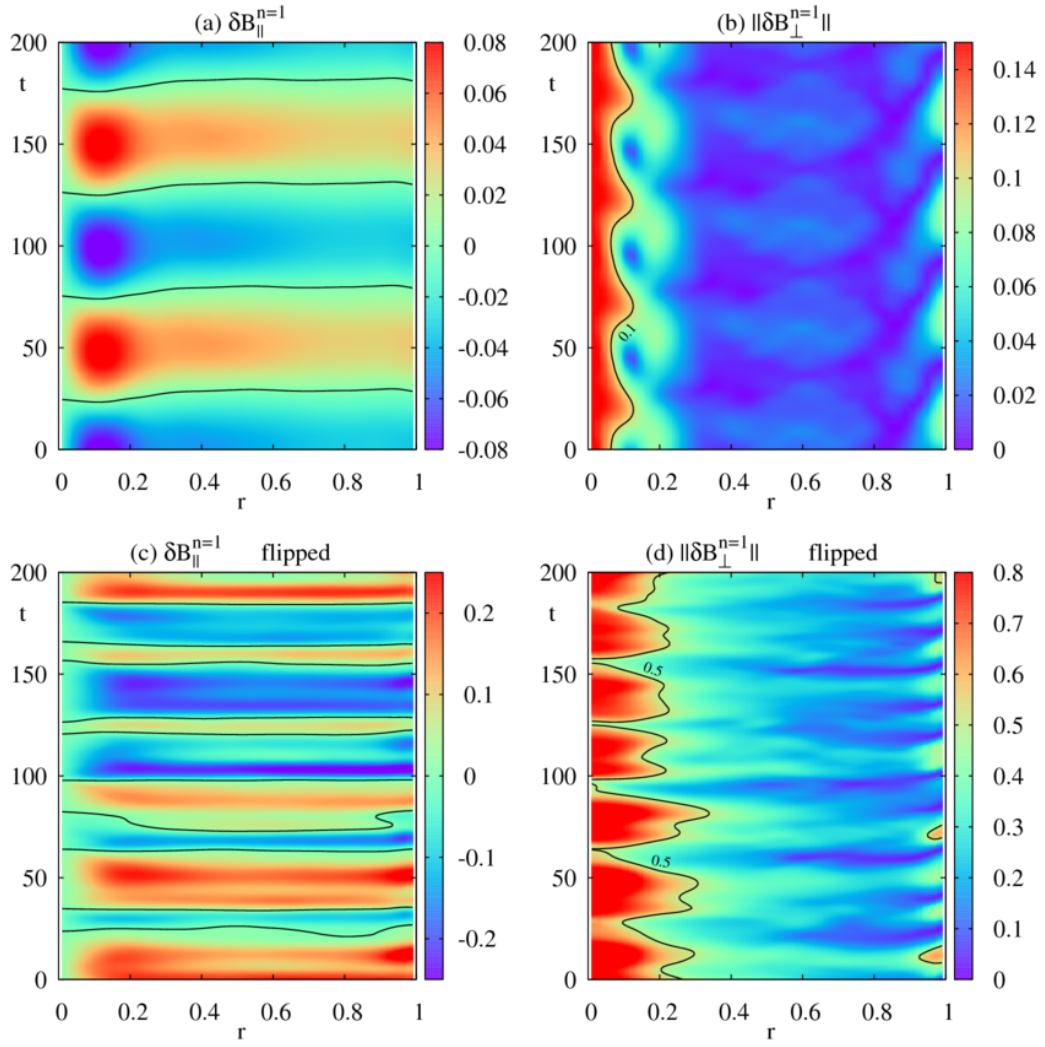

Figure 8: Parallel and perpendicular $n = 1$ magnetic fluctuations. The radial dependence, at the height of the magnetic axis, for 200 Alfvén times during sustainment, is shown. Coherent structures are observed only for the regular configuration.

The parallel and perpendicular magnetic fluctuation components with toroidal dependence $n = 1$ are shown in Fig. 8. The radial dependence , at the height of the magnetic axis, for 200 Alfvén times during sustainment, is shown. A coherent spatio-temporal oscillation is clearly observed for the regular case. This produces the rotation of the kink-distorted central open flux column (García Martínez and Farengo, 2010). For the flipped case, a much larger level of fluctuations without such a coherent behavior is observed. In this case, the parallel fluctuation is (roughly) a factor 3 larger than that of the regular case. The difference in the perpendicular fluctuation is even larger and close to a factor 5 (again, compared to that of the regular case).

The Ohm's law in Eq. (6) indicates that the ideal part of the electric field is always perpendicular to $\mathbf{B}$. Thus, we would have only the resistive decay acting on the configuration. The dynamics of the MHD fluctuations during relaxation induces a net electric field along the mean magnetic configuration. This is captured by the dynamo electric field.

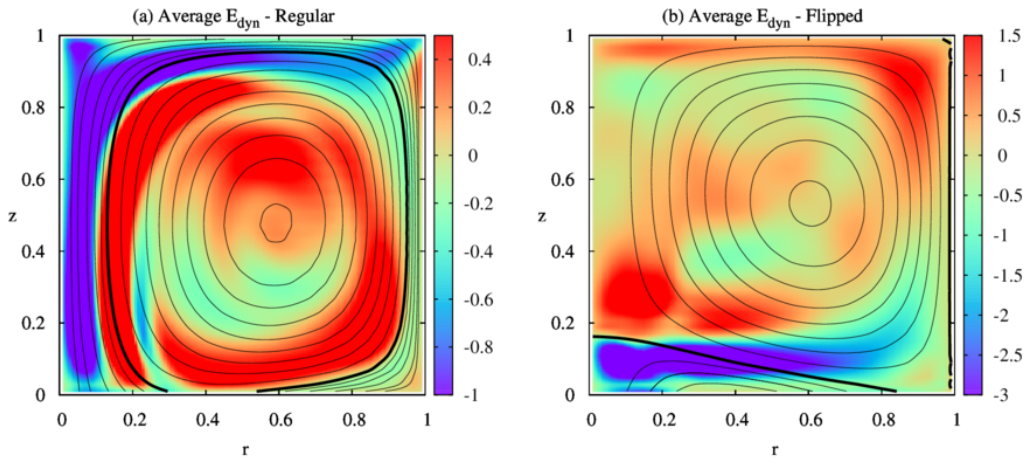

Figure 9: Average dynamo electric field.

The parallel component of the MHD dynamo field is usually expressed as $E_{dyn} = \langle \mathbf{u} \times \mathbf{B} \rangle \cdot \mathbf{B}^{n=0}/B$, where $\mathbf{u}$ and $\mathbf{B}$ are the fluctuating velocity and magnetic field in the plasma, $\mathbf{B}^{n=0}$ is the mean magnetic field and $\langle \cdot \rangle$ denotes, in this case, temporal averaging. Fig. 9 shows E_{dyn}, averaged during sustainment for both cases. As measured by Al-Karkhy et al. (1993) for the regular case, we observe a strong antidynamo/dynamo structure in the central flux column (antidynamo means that E_{dyn} is antiparallel to $\mathbf{B}^{n=0}$). This the basis of the toroidal current drive mechanism induced by relaxation (which is equivalent to the poloidal flux amplification process). Up to our knowledge, the dynamo action during the sustainment of the flipped configuration has not been studied before. Fig. 9 (b) shows the mean E_{dyn} for the flipped configuration. In this case, the strong antidynamo is placed at the bottom of the flux conserver, mainly (but not exclusively) located in the open flux region. A strong dynamo appears close to the separatrix in the closed flux region. In agreement with the larger level of fluctuations observed, a stronger dynamo action is present in the flipped configuration. This is the kind of conclusions that one can only obtain by studying the dynamics of relaxation, since the original theory does not describe the behavior of the fluctuations.

5 CONCLUSIONS

A numerical study of the dynamics of magnetic relaxation of driven configurations inside a cylindrical flux conserver was presented. The theory of driven configurations was briefly introduced. The saturated states were classified as regular (below resonance) and flipped (above resonance) spheromaks. Simulation of the sustainment phase of the regular configuration was achieved using both the vacuum magnetic field as well as the axisymmetric relaxed state with $\lambda = 4.855 < \lambda_1$. On the other hand, the sustainment phase of the flipped configuration, beginning from the relaxed state with $\lambda = 5.035 > \lambda_1$, was also demonstrated. Up to the best of our knowledge, these are the first results regarding the dynamics of flipped configurations.

The most relevant results may be summarized as follows. For the same helicity injection rate, the sustainment of the flipped configuration involves a larger level of fluctuations than the regular case. The difference was found to be larger than one order of magnitude in the magnetic energy, around a factor 3 for the parallel magnetic fluctuation and around a factor 5 for the perpendicular magnetic fluctuation ($n = 1$ at the height of the magnetic axis). A spatio-temporal coherent structure was observed for the regular case (which is responsible for the almost rigid rotation of the central column), but no coherence was found for the flipped configuration. Thus, no coherent large-scale structures are expected in the latter case. Also the instantaneous toroidally averaged ($n = 0$) magnetic field profiles exhibit a larger dispersion in the flipped case than in the regular case. The local $\lambda(\psi)$ profiles along the poloidal plane show a large dispersion in the open flux region and in the vicinity of the separatrix for both cases. In the interior flux surfaces both configurations remain remarkably close to the marginally stable linear $\lambda(\psi)$ profile.

We have reported on the dynamics of sustainment of configurations on both sides of the resonant relaxed state. These results suggest that the regular configuration is preferably from the point of view of the level of fluctuations required. But more in general, this work proves that the dynamics of sustainment via magnetic relaxation in helicity injected devices is strongly affected by the topology of the equilibrium configuration.

REFERENCES

Al-Karkhy A., Browning P.K., Cunningham G., Gee S.J., and Rusbridge M.G. Observations of the magnetohydrodynamic dynamo effect in a spheromak plasma. *Physical Review Letters*, 70:1814–1817, 1993.

Barnes C.W., Fernández J.C., Henins I., Hoida H.W., Jarboe T.R., Knox S.O., Marklin G.J., and McKenna K.F. Experimental determination of the conservation of magnetic helicity from the balance between source and spheromak. *Physics of Fluids*, 29:3415–3432, 1986.

Bellan P.M. *Spheromaks*. Imperial College Press, London, 2000.

Brennan D.P., Browning P.K., and van der Linden R.A.M. A two-dimensional magnetohydrodynamic stability model for helicity-injected devices with open flux. *Physics of Plasmas*, 9:3526–3535, 2002.

Cowling T.G. The stability of gaseous stars. *Monthly Notices of the Royal Astronomical Society*, 94:768–782, 1934.

Finn J.M. and Antonsen T.M. Magnetic helicity: what it is, and what it is good for? *Comments Plasma Physics and Controlled Fusion*, 33:1139–+, 1985.

Forrer H. and Jeltsch R. A higher-order boundary treatment for cartesian-grid methods. *Journal of Computational Physics*, 140:259–277, 1998.

García Martínez P.L. *Dynamics of Magnetic Relaxation in Spheromaks, Topics in Magnetohy-*

drodynamics, ISBN: 978-953-51-0211-3. InTech, 2012. doi:10.5772/35534.

García Martínez P.L. and Farengo R. Non-linear dynamics of kink-unstable spheromak equilibria. *Physics of Plasmas*, 16:082507, 2009a.

García Martínez P.L. and Farengo R. Relaxation of spheromak configurations with open flux. *Physics of Plasmas*, 16:112508, 2009b.

García Martínez P.L. and Farengo R. Spheromak formation and sustainment by tangential boundary flows. *Physics of Plasmas*, 17:050701, 2010.

Hasegawa A. Self-organization processes in continuous media. *Advances in Physics*, 34:1–42, 1985.

Heyvaerts J. and Priest E.R. Coronal heating by reconnection in DC current systems - A theory based on Taylor's hypothesis. *Astronomy and Astrophysics*, 137:63–78, 1984.

Jarboe T.R. The spheromak confinement device. *Physics of Plasmas*, 12(5):058103–+, 2005.

Jensen T.H. and Chu M.S. Current drive and helicity injection. *Physics of Fluids*, 27:2881–2885, 1984.

Knox S.O., Barnes C.W., Marklin G.J., Jarboe T.R., Henins I., Hoida H.W., and Wright B.L. Observations of spheromak equilibria which differ from the minimum-energy state and have internal kink distortions. *Physical Review Letters*, 56:842–845, 1986.

Powell K.G., Roe P.L., Linde T.J., Gombosi T.I., and de Zeeuw D.L. A Solution-Adaptive Upwind Scheme for Ideal Magnetohydrodynamics. *Journal of Computational Physics*, 154:284–309, 1999.

Roe P.L. Approximate Riemann Solvers, Parameter Vectors, and Difference Schemes. *Journal of Computational Physics*, 43:357–+, 1981.

Rosenbluth M.N. and Bussac M.N. MHD stability of Spheromak. *Nuclear Fusion*, 19:489–498, 1979.

Taylor J.B. Relaxation of Toroidal Plasma and Generation of Reverse Magnetic Fields. *Physical Review Letters*, 33:1139–1141, 1974.

Taylor J.B. Relaxation and magnetic reconnection in plasmas. *Reviews of Modern Physics*, 58:741–763, 1986.

Toth G. The $\nabla \cdot \mathbf{B} = 0$ Constraint in Shock-Capturing Magnetohydrodynamics Codes. *Journal of Computational Physics*, 161:605–652, 2000.

Woltjer L. A Theorem on Force-Free Magnetic Fields. *Proceedings of the National Academy of Science*, 44:489–491, 1958.